Laminar film condensation along a vertical plate embedded in an anisotropic porous medium with oblique principal axes

Gérard Degan, Arthur Sanya & Christian Akowanou

Heat and Mass Transfer
Wärme- und Stoffübertragung

ISSN 0947-7411

Heat Mass Transfer
DOI 10.1007/s00231-015-1684-2

Springer

Heat Mass Transfer
DOI 10.1007/s00231-015-1684-2

ORIGINAL

Laminar film condensation along a vertical plate embedded in an anisotropic porous medium with oblique principal axes

Gérard Degan[1] · **Arthur Sanya**[1] · **Christian Akowanou**[1]

Received: 1 October 2014 / Accepted: 15 September 2015

Abstract This work analytically investigates the problem of steady film condensation along a vertical surface embedded in an anisotropic porous medium filled with a dry saturated vapor. The porous medium is anisotropic in permeability whose principal axes are oriented in a direction which is oblique to the gravity vector. On the basis of the generalized Darcy's law and within the boundary layer approximations, similar solutions have been obtained for the temperature and flow patterns in the condensate. Moreover, closed form solutions for the boundary layer thickness and heat transfer rate have been obtained in terms of the governing parameters of the problem.

List of symbols

a, b, c	Constants
c_P	Specific heat capacity of fluid at constant pressure
Da	Darcy number
f	Dimensionless stream function
g	Gravitational acceleration
h_{fg}	Latent heat of condensation
h_x	Local convective heat transfer coefficient
Ja	Jacob number
$\overline{\overline{K}}$	Flow permeability tensor
K_1, K_2	Flow permeability along the principal axes
K^*	Anisotropic permeability ratio, K_1/K_2
k	Effective thermal conductivity of the liquid film
L	Height of the surface
Nu_x	Local Nusselt number
q	Local heat transfer rate
Ra_L	Rayleigh number
Ra_x	Local Rayleigh number
T	Temperature
V	Velocity of the liquid film in the porous medium
u, v	Velocity components in x, y directions
P	Pressure
x, y	Cartesian coordinates
W	The width of the plate

Greek symbols

α	Thermal diffusivity
δ_L	Liquid film thickness
η	Similarity variable
θ	Dimensionless temperature profile
ΔT	Characteristic scale of temperature, $T_S - T_w$
μ	Dynamic viscosity of the fluid (kg m $^{-1}$ s^{-1})
Γ	Dimensionless total mass rate of condensate
Ψ	Stream function
ρ	Density of the fluid
Φ	Orientation angle of principal axes

Superscript

*	Dimensional quantities

Subscripts

∞	Refers to condition at infinity
e	Refers to effective properties due to the presence of the porous domain
L	Refers to liquid region
s	Refers to saturated properties
w	Refers to the vertical surface

✉ Gérard Degan
ger_degan@yahoo.fr

[1] Laboratoire d'Energétique et de Mécanique Appliquées (LEMA), Ecole Polytechnique d'Abomey-Calavi (EPAC), Université d'Abomey-Calavi (UAC), Boite Postale 2009, Cotonou, Benin

Published online: 08 December 2015

1 Introduction

The problem of film condensation phenomena with the presence of convection in a porous medium occurs in various fields of science and engineering. Common examples are heat and fluid flow for some industrial drying and cooling processes, packed-bed heat exchangers, steam injection petroleum recovery, solidification of castings, porous enhanced heat transfer surfaces, geothermal reservoirs, and many others where the problem of two-phase in a porous medium involving phase change have important applications. And when two phase flow exists in a porous medium, it is known that Darcy's law is also applicable to both the liquid and the vapor phases provided that the concept of relative permeability be introduced. This is to account for the fact that the pore spaces are filled partly with vapor and partly with steam. This problem based on the standard approximations used in the classical film condensation was first formulated by Cheng [1] along an inclined cooled plate embedded in a Darcian porous medium by means of similarity transformation. Assuming that the condensate and the vapor are separated by a distinct boundary with no two-phase zone and that the condensate film is thin and has constant properties, Cheng [1] obtained closed-form expressions of the Nusselt number in terms of the Rayleigh number and the boundary layer thickness of the condensate. An analytical solution for the problem of film condensation in porous medium with non-zero lateral mass flux at the boundary wall is presented by Liu et al. [2]. The analysis was later extended by Kimura and Bejan [3] to a frustum of a cone without transverse curvature effect. Wang and Tu [4] studied the effect of non-condensable gas on forced convection condensation along a horizontal plate embedded in a porous medium. Renken et al. [5] numerically examinated the effects of vapor velocity on film condensation along a surface embedded in a porous medium and the results obtained provide valuable fundamental predictions which can be used in a number of industrial applications. Also, an analytical approach to solve the laminar film condensation outside a horizontal elliptical tube embedded in a porous medium was performed by Chiou and Chang [6]. Closed-form expressions for the condensate film thickness, the condensate flow rate and the heat transfer coefficient have been obtained by Al-Nimr and Alkam [7] for the problem of film condensation over a vertical plate embedded in a porous medium. Under steady state conditions, the state of the art can be found in Nield and Bejan [8] and Kaviany [9].

A few studies have also been reported for the case of the conjugate laminar film condensation on the external sides of the vertical plate embedded in a homogeneous porous medium. Char et al. [10] have investigated the conjugate mixed-convection laminar film condensation along a conducting vertical plate in a porous medium filled with dry saturated vapor. Using a cubic spline collocation method to solve this conjugate heat transfer problem, these authors have obtained results of interest to highlight the influence of the wall conduction. This work is extended by Bautista et al. [11] by studying analytically and numerically the conjugate heat transfer film-condensation process of a saturated vapor on a vertical conducting fin immersed in a porous medium, considering that the base of the fin is found at temperature lower than the temperature of saturated-vapor porous medium. It has been found that this boundary condition can modify the results obtained in previous works, where the effect of the longitudinal heat conduction through the fin has been neglected.

In all the above studies the porous media were assumed to be isotropic whereas, in several applications, the porous materials are anisotropic. Despite this fact, natural convection in such anisotropic porous media has received relatively little attention. The effects of an anisotropic permeability on thermal convection in a porous medium began with the investigation of Castinel and Combarnous [12], concerning the onset of motion in a horizontal layer heated from below, and continued with the works of Epherre [13], Kvernvold and Tyvand [14] and Nilsen and Storesletten [15]. Natural convection within enclosures heated from the side was investigated by Kimura et al. [16] and Ni and Beckermann [17], for the case when one of the principal axes of anisotropy of permeability is aligned with gravity and by Zhang et al. [18], Degan et al. [19] and Degan and Vasseur [20] when the principal axes are inclined with respect to gravity. It was demonstrated by these authors that the effects of the anisotropy considerably modify the convective heat transfer. Recently, the effects of anisotropy on the boundary-layer free convection over an impermeable vertical plate, for the case when one of the principal axes of anisotropy is along the plate, were investigated by Ene [21], using the method of integral relations. It was concluded that, if the permeability in the direction normal to the plate is greater than the permeability along the plate, then there is an increase in the temperature field. This investigation was extended by Vasseur and Degan [22] for the case when the porous medium is anisotropic in permeability with its principal axes oriented in a direction that is oblique to the gravity vector. Within the framework of boundary-layer approximations, similarity solutions are obtained for the case where wall temperature varies as a power function of distance from the leading edge. Solving numerically the full governing equations by using a finite-difference procedure, these authors demonstrated that the anisotropic parameters greatly influence the local heat transfer rates.

The present work is devoted to the study of convection laminar film condensation along a vertical plate embedded

in a fluid saturated porous medium filled with a dry saturated vapor. The porous medium is anisotropic in permeability with its principal axes oriented in a direction that is oblique to the gravity vector. Assuming the usual approximations used in the classical film condensation problems, a similarity solution for the problem is found. Consequently, closed-form expressions of the heat transfer rates and the boundary layer thickness of the condensate are obtained in terms of the Rayleigh number and the anisotropic parameters.

2 Mathematical formulation

Consider the problem of steady cooling at temperature T_w of a vertical plate of length L embedded in a fluid saturated porous medium filled with a dry saturated vapor. Condensation of the saturated vapor at constant temperature T_S (corresponding to its pressure) is expected to occur along the hot impermeable plate and inside the porous medium. If the wall temperature (T_w) is less than the saturated temperature (T_S), a film of condensate (liquid) will form adjacent to the plate and flows downward because of gravity. The porous medium is anisotropic in permeability with its principal axes oriented in a direction that is oblique to the gravity vector. The physical model and coordinate system are shown in Fig. 1. The x and y axes are aligned with the vertical and the horizontal directions respectively. The permeability along the two principal axes of the porous matrix are denoted by K_1 and K_2. The anisotropy of the porous medium is characterized by the permeability ratio $K^* = K_1/K_2$ and the orientation angle φ, defined as the angle between the horizontal direction and the principal axis with the permeability K_2.

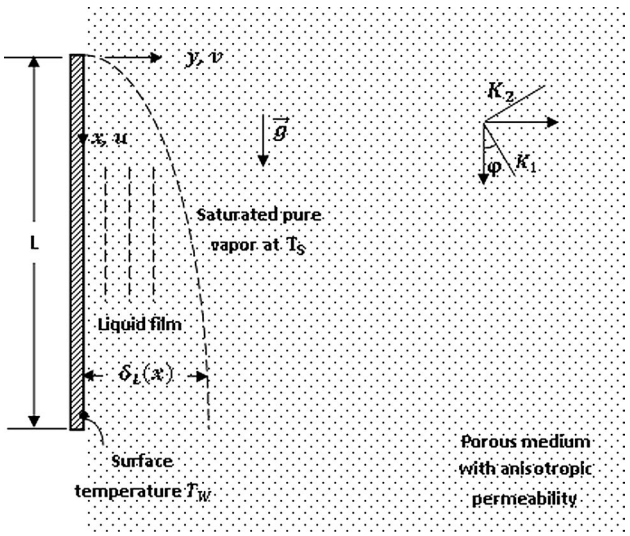

Fig. 1 Physical model and coordinate system

The condensate and the dry saturated vapor are separated by a distinct interface at $y = \delta_L$. The condensate film is thin such that the boundary layer approximations can be applied. The flow is steady, laminar, incompressible and two dimensional. The porous medium is saturated with an incompressible viscous fluid that is in local thermodynamic equilibrium with the solid matrix. The Boussinesq approximation is applicable. Capillarity is negligible. Darcy's law is applicable to both the dry vapor and liquid phases in the porous medium.

Under the aforementioned assumptions, the Darcy system of equations describing the problem of convective laminar film condensation in an anisotropic porous medium (for the condensate film) can be written as follows [23]:

$$\nabla \cdot \vec{V} = 0 \tag{1}$$

$$\vec{V} = \frac{\overline{\overline{K}}}{\mu}(-\nabla P + \rho\vec{g}) \tag{2}$$

$$\vec{V} \cdot \nabla T = \alpha \nabla^2 T \tag{3}$$

In these equations, $\vec{V}$ denotes the velocity vector, p the pressure and T the temperature for the condensate and $\vec{g}$ the gravitational acceleration. Moreover, μ is the dynamic viscosity, ρ the density and $\alpha = (k/(\rho c_p)_f)$ is the thermal diffusivity, where $(\rho c_p)_f$ is the volumetric heat capacity of the fluid and c_p is the specific heat of the fluid, k is the effective thermal conductivity. The symmetrical second order permeability tensor $\overline{\overline{K}}$ is defined as [19]:

$$\overline{\overline{K}} = \begin{bmatrix} K_1 sin^2\varphi + K_2 cos^2\varphi & (K_2 - K_1) sin\varphi cos\varphi \\ (K_2 - K_1) sin\varphi cos\varphi & K_2 sin^2\varphi + K_1 cos^2\varphi \end{bmatrix} \tag{4}$$

In the coordinate system (Ox, Oy), the previous governing Eqs. (1)–(3) can be rewritten in physical variables as follows:

$$\frac{\partial u}{\partial x} + \frac{\partial v}{\partial y} = 0 \tag{5}$$

$$au - cv = \frac{K_1}{\mu}\left(-\frac{\partial P}{\partial x} + \rho g\right) \tag{6}$$

$$-cu + bv = -\frac{K_1}{\mu}\frac{\partial P}{\partial y} \tag{7}$$

$$u\frac{\partial T}{\partial x} + v\frac{\partial T}{\partial y} = \alpha\left(\frac{\partial^2 T}{\partial x^2} + \frac{\partial^2 T}{\partial y^2}\right) \tag{8}$$

where

$$\begin{cases} a = cos^2\varphi + K^* sin^2\varphi \\ b = sin^2\varphi + K^* cos^2\varphi \\ c = (1 - K^*) sin\varphi cos\varphi \end{cases} \tag{9}$$

Eliminating the pressure term between the Eqs. (6) and (7), one can obtain the momentum equation which becomes:

$$a\frac{\partial^2\psi}{\partial y^2}+2c\frac{\partial^2\psi}{\partial x\partial y}+b\frac{\partial^2\psi}{\partial x^2}=\frac{K_1}{\mu_L}g\frac{\partial\rho}{\partial y} \tag{10}$$

In the above equation, ψ is the stream function related to the velocity components by:

$$u=\frac{\partial\psi}{\partial y},\quad v=-\frac{\partial\psi}{\partial x} \tag{11}$$

so that the continuity Eq. (1) is automatically satisfied.

We consider now the boundary layer regime for which most of the liquid film is restricted to a thin layer along the vertical axis directed updown, i.e. when $y<\delta_L$. In this situation, one can observe that $\partial^2/\partial x^2,\ \partial^2/(\partial x\partial y)\ll\partial^2/\partial y^2$. Consequently, from the momentum Eq. (10), it is clear that a boundary layer regime is possible only when the second and the third terms, on the left-hand side of the equation can be neglected when compared with the first one, i.e. when the following conditions:

$$a\frac{\partial^2\psi}{\partial y^2}\gg c\frac{\partial^2\psi}{\partial x\partial y} \tag{12}$$

and

$$a\frac{\partial^2\psi}{\partial y^2}\gg b\frac{\partial^2\psi}{\partial x^2} \tag{13}$$

are satisfied. So, under the boundary layer approximations, the governing Eqs. (10) and (8) in an anisotropic porous medium are given as follows:

$$a\frac{\partial\psi}{\partial y}=\frac{K_1}{\mu_L}g(\rho_L-\rho_v) \tag{14}$$

$$\frac{\partial^2T_L}{\partial y^2}=\frac{1}{\alpha_L}\left(\frac{\partial\psi_L}{\partial y}\frac{\partial T_L}{\partial x}-\frac{\partial\psi_L}{\partial x}\frac{\partial T_L}{\partial y}\right) \tag{15}$$

In the above equation, the subscript L and v denotes the quantities associated with the liquid and the saturated vapor phases respectively.

3 Scale analysis and validity of the film condensation boundary layer

Consider the condensate film, i.e. the liquid layer near the plate as the slender boundary-layer region ($\delta_L\times L$) with $\delta_L\ll L$, where δ_L is the boundary layer thickness defined as the order of magnitude of the distance in which the horizontal velocity v changes from 0 to v_L. That region is distinct from the immense domain of the porous medium occupied by the saturated vapor. Thus, in that space, the following scales for in x, y and v are:

$$x\sim L,\quad y\sim\delta_L,\quad v\sim v_L \tag{16}$$

In the $\delta_L\times L$ region, the mass continuity Eq. (5) and the momentum Eq. (14) require the following balances:

$$\frac{u_L}{L}\sim\frac{v_L}{\delta_L} \tag{17}$$

$$u_L\sim\frac{K_1}{\mu_L}g(\rho_L-\rho_v) \tag{18}$$

For the boundary layer flow in the liquid film, the energy Eq. (8) becomes:

$$u_L\frac{\partial T_L}{\partial x}+v_L\frac{\partial T_L}{\partial y}=\alpha_L\frac{\partial^2T_L}{\partial y^2} \tag{19}$$

Following Bejan [24], the scaling law implied by the energy Eq. (19) is more visible if it is integrated from $y=0$ to $y=\delta_L$.

$$\rho c_p\left[(v_LT_L)_{y=\delta_L}+\frac{d}{dx}\int_0^{\delta_L}u_LT_Ldy\right]=\left(k\frac{\partial T_L}{\partial y}\right)_{y=\delta_L}-\left(k\frac{\partial T_L}{\partial y}\right)_{y=0} \tag{20}$$

In the $\delta_L\times L$ region, the equation of energy (20) accounts for the competition between four terms and their respective scales are:

$$\begin{aligned}&\left(\rho c_pv_L\Delta T\right)\ or\ \left(\rho c_p\frac{u_L\Delta T\delta_L}{L}\right)\\&\sim\left(\rho v_Lh_{fg}\right)\ or\ \left(k\frac{\Delta T}{\delta_L}\right)\end{aligned} \tag{21}$$

where $\Delta T=T_s-T_w$ and h_{fg} is the latent heat of condensation. The (ρv_Lh_{fg}) scale is associated with the heating of the interface through the condensation of saturated vapor, which is entrained with velocity v_L into the liquid film. In conclusion, the energy balance (19) requires:

$$\left(k\frac{\Delta T}{\delta_L}\right)\sim\left(\rho v_Lh_{fg}\right)\ or\ \left(\rho c_pv_L\Delta T\right) \tag{22}$$

Determining three unknown scales for (u_L, v_L, δ_L) from the three Eqs. (17), (18) and (22), one can obtain what follows:

$$u_L\sim\frac{\alpha_L}{L}Ra_L \tag{23}$$

$$v_L\sim\frac{\alpha_L}{L}Ra_L^{1/2} \tag{24}$$

$$\delta_L\sim\left(\frac{1}{Ra_L}\right)^{1/2}L \tag{25}$$

where

$$Ra_L = \frac{K_1 g L(\rho_L - \rho_v)}{\alpha_L \mu_L} \tag{26}$$

is the film Rayleigh number based on permeability K_1. Consequently, the scale of steam function ψ_L can be termed as:

$$\psi_L \sim \alpha_L Ra_L^{1/2} \tag{27}$$

Following Ene and Polievski [25], taking into account to Eqs. (12), (13) and (27), it follows that the conditions:

$$\frac{a}{c}\frac{L}{\delta_L} \gg 1 \tag{28}$$

and

$$\frac{a}{b}\frac{L^2}{\delta_L^2} \gg 1 \tag{29}$$

must be satisfied.

Equations (28) and (29) indicate that, if $a/c = 0(1)$ and $a/b = 0(\delta_L/L)$, the boundary layer hypothesis cannot be used. However, if $a/c = 0(\delta_L/L)$ and $a/b = 0\left(\delta_L^2/L^2\right)$, then the terms of the left hand side of Eq. (10) are the same order of magnitude and the boundary layer approximations can be involved.

4 Resolution

In the boundary layer regime, i.e. when conditions (28) and (29) are satisfied, it can be readily demonstrated that Eqs. (14) and (15) are required to satisfy the following boundary conditions:

- At the plate:

$$y = 0: \quad v_L = -\frac{\partial \psi}{\partial x} = 0, \quad T_L = T_w \tag{30}$$

- At the liquid–vapor interface at $y = \delta_L$, the continuity of temperature, mass flux and energy flux are:

$$y = \delta_L: \quad T_L = T_s \tag{31}$$

$$y = \delta_L: \quad \dot{m} = \rho_L \left(\frac{\partial \psi_L}{\partial y}\frac{d\delta_L}{dx} + \frac{\partial \psi_L}{\partial x} \right) \tag{32}$$

$$y = \delta_L: \quad \dot{m} h_{fg} = -k_p \left(\frac{\partial T_L}{\partial y} \right) \tag{33}$$

where $\dot{m}$ is the mass flux of the liquid across the interface, h_{fg} is the latent heat at T_s and k_p is the thermal conductivity of the porous medium saturated with liquid. Substituting Eqs. (32) into (33) gives the following interface condition:

$$y = \delta_L: \quad h_{fg}\rho_L \left(\frac{\partial \psi_L}{\partial y}\frac{d\delta_L}{dx} + \frac{\partial \psi_L}{\partial x} \right) = k_p \left(\frac{\partial T_L}{\partial y} \right) \tag{34}$$

As suggested by the previous boundary layer scales, we can introduce the following similarity transformations:

$$\eta_{x,L} = \frac{y}{x} Ra_{x,L}^{1/2} \tag{35}$$

$$\psi_L = \alpha_L Ra_{x,L}^{1/2} f_L(\eta_{x,L}) \tag{36}$$

$$\theta_L(\eta_{x,L}) = \frac{T_L - T_S}{T_W - T_S} \tag{37}$$

where $Ra_{x,L} = K_1 g(\rho_L - \rho_v)x/(\mu_L \alpha_L)$ is the local Rayleigh number of the liquid film.

Using Eqs. (35)–(37), the governing Eqs. (14) and (15) can be transformed into the following set of ordinary differential equations:

$$f_L' = \frac{1}{a} \tag{38}$$

$$\theta_L'' + \frac{1}{2} f_L \theta_L' = 0 \tag{39}$$

where the primes denote differentiation with respect to $\eta_{x,L}$.

The above system is subject to the boundary conditions at the plate:

$$f_L(0) = 0, \quad \theta_L(0) = 1 \tag{40}$$

while the boundary conditions at interface (where $y = \delta_L$) yield:

$$\theta_L(\eta_{L\delta}) = 0 \tag{41}$$

and

$$Ja\theta_L'(\eta_{L\delta}) = -\frac{1}{2} f_L(\eta_{L\delta}) \tag{42}$$

where $Ja = c_{pL}(T_s - T_w)h_{fg}$ is the well-known Jacob number which corresponds to a mesure of degree of wall subcooling, and the dimensionless liquid film thickness yields:

$$\eta_{L\delta} = \left(\eta_{x,L}\right)_{y=\delta_L} = \frac{\delta_L}{x} Ra_{x,L}^{1/2} \tag{43}$$

Solving the above system of equations, we obtain the following exact solutions:

$$f_L(\eta_{x,L}) = \frac{\eta_{x,L}}{a} \tag{44}$$

$$\theta_L(\eta_{x,L}) = 1 - \frac{erf\left(\frac{\eta_{x,L}}{2\sqrt{a}}\right)}{erf\left(\frac{\eta_{L\delta}}{2\sqrt{a}}\right)} a \tag{45}$$

where $\eta_{L\delta}$ is determined from the following expression of Ja:

$$Ja = \sqrt{\pi}\frac{\eta_{L\delta}}{2\sqrt{a}} exp\left(\frac{\eta_{L\delta}^2}{4a}\right) erf\left(\frac{\eta_{L\delta}}{2\sqrt{a}}\right) \tag{46}$$

The above result, in case of constant permeability, (i.e. $K^* = 1$) reduces to that of Cheng [1] for isotropic porous medium.

We consider now the situation for which the flow field in the vapor phase at $y > \delta_L$. For this case, it is noticed that, since the temperature T_s in the vapor phase is constant, the energy equation is automatically satisfied. Making use of continuity equation and considering the boundary layer approximations applied to the generalized Darcy's law, one can write:

$$u_v = 0, \quad v_v = g(x) \tag{47}$$

From the mass continuity equation at the interface, it is convenience to write:

$$\dot{m} = \rho_v\left(u_v\frac{d\delta_v}{dx} - v_v\right)_{y=\delta_L} = \rho_L\left(u_L\frac{d\delta_L}{dx} - v_L\right)_{y=\delta_L} \tag{48}$$

and making use of Eqs. (35), (36), (43), (44) and (48), one obtains:

$$\dot{m} = \frac{1}{2}\frac{\rho_L\alpha_L}{x}\frac{Ra_{x,L}}{a}\frac{\delta_L}{x} \tag{49}$$

which becomes, in dimensionless terms, the mass flux of the liquid flow across the interface as follows:

$$\dot{M} = \frac{\dot{m}x}{\rho_L\alpha_L} = \frac{Ra_{x,L}}{2a}\frac{\delta_L}{x} = \frac{1}{2}\frac{Ra_{x,L}^{1/2}}{a}\eta_{L\delta} \tag{50}$$

By defining the velocity in the vapor phase far away from the liquid film and with the aid of Eq. (49), one can obtain in the same way:

$$v_v = -\frac{\dot{m}}{\rho_\infty} = -\frac{1}{2}\frac{\rho_L}{\rho_\infty}\frac{\alpha_L}{x}\frac{Ra_{x,L}}{a}\frac{\delta_L}{x} \tag{51}$$

Accordingly, the dimensionless velocity in the vapor region can be termed as:

$$V_v = \frac{v_v x}{\alpha_L} = -\frac{1}{2}\frac{\rho_L}{\rho_\infty}\frac{Ra_{x,L}}{a}\frac{\delta_L}{x} = -\frac{1}{2}\frac{\rho_L}{\rho_\infty}\frac{Ra_{x,L}^{1/2}}{a}\eta_{L\delta} \tag{52}$$

which shows obviously that the vapor flow field is moving toward the interface, in the direction opposite to that of the system coordinate. As consequence, the total mass rate of condensate along the plate at a given distance x from the origin of coordinate axes can be defined as:

$$\gamma = \int_0^x W\dot{m}dt \tag{53}$$

where W is the width of the plate. Making use of Eqs. (49) and (50), the dimensionless total mass rate of condensate along the vertical surface, at the position x from the origin, can be calculated by the following expression:

$$\Gamma = \frac{\gamma}{\alpha_L\rho_L} = \frac{W}{2}\frac{Ra_{x,L}}{a}\frac{\delta_L}{x} = \frac{W}{2}\frac{Ra_{x,L}^{1/2}}{a}\eta_{L\delta} \tag{54}$$

The surface heat flux along the impermeable surface is defined as:

$$q_w = -k_{m,L}\left(\frac{\partial T_L}{\partial y}\right)_{y=0} = k_{m,L}(T_W - T_S)\frac{Ra_{x,L}^{1/2}}{x}\left[-\theta_L'(0)\right] \tag{55}$$

where $k_{m,L}$ is the thermal conductivity of the porous medium saturated with liquid. Taking into account Eqs. (45), (55) becomes:

$$q_w = \left(\frac{Ra_{x,L}}{a\pi}\right)^{1/2}\frac{k_{m,L}(T_W - T_S)}{xerf\left(\frac{\eta_{L\delta}}{2a^{1/2}}\right)} \tag{56}$$

The local heat transfer rate defined as the local Nusselt number is expressed as follows:

$$Nu_x = \frac{hx}{k_{m,L}} = \frac{q_w x}{k_{m,L}(T_W - T_S)} \tag{57}$$

where h is the local heat transfer coefficient. Substituting Eqs. (56) into (57), one can obtain:

$$\frac{Nu_x}{Ra_{x,L}^{1/2}} = \frac{1}{(\pi a)^{1/2} erf\left(\frac{\eta_{L\delta}}{2\sqrt{a}}\right)} \tag{58}$$

It is obvious that the precedent result (Eq. 58) is an exact solution for the local Nusselt number in terms of the dimensionless boundary layer thickness and of the anisotropic parameters of the saturated porous medium. Moreover, the expression of Nu_x is implicity a function of the dimensionless degree of wall subcooling calculated by Eq. (45). It is also noticed that, in the case of the saturated isotropic porous medium for which $K^* = 1$ (i.e. for $a = 1$), the result obtained for Nu_x is in agreement with that found in the past by Cheng [1].

As pointed out by Cheng [1], we will consider now both the limiting cases, one for the weakened boundary layer thickness (i.e. with $\eta_{L\delta} \to 0$), and the other for the larger boundary layer thickness corresponding to $\eta_{L\delta} \to \infty$.

1. As $\eta_{L\delta} \to 0$, one can obtain from Eqs. (45) and (46) that:

$$\eta_{L\delta} = \sqrt{2aJa} \tag{59}$$

which depends on the anisotropic parameters of the porous structure and shows that, for any value of the coefficient a, that $Ja \to 0$ as $\eta_{L\delta} \to 0$. Consequently, the temperature distribution of the condensate liquid can be expressed as follows:

$$\theta_L(\eta_{x,L}) = 1 - \frac{\eta_{x,L}}{\sqrt{2aJa}} \tag{60}$$

Similarly, in this limiting case, both the local heat transfer rate and the film boundary layer thickness can be expressed as:

$$\frac{Nu_x(2Ja)^{1/2}}{Ra_{x,L}^{1/2}} = \left(\frac{1}{a}\right)^{1/2} \tag{61}$$

and

$$\frac{\delta_L}{x} = \left(\frac{2aJa}{Ra_{x,L}}\right)^{1/2} \tag{62}$$

respectively.

2. As $\eta_{L\delta} \to \infty$, one can obtain from Eqs. (45) and (46) that:

$$\theta_L(\eta_{x,L}) = 1 - \mathrm{erf}\left(\frac{\eta_{x,L}}{2\sqrt{a}}\right) \tag{63}$$

Similarly, in this limiting case, the local heat transfer rate can be expressed as:

$$\frac{Nu_x}{Ra_{x,L}^{1/2}} = \left(\frac{1}{\pi a}\right)^{1/2} \tag{64}$$

and

$$Ja = \sqrt{\pi}\frac{\eta_{L\delta}}{2\sqrt{a}} exp\left(\frac{\eta_{L\delta}^2}{4a}\right) \tag{65}$$

Following Cheng [1], Eqs. (61) and (64) suggest that it is convenient to present $Nu_x(2Ja)^{1/2}/Ra_{x,L}^{1/2}$ in terms of $(2Ja)^{1/2}$ which can be obtained by first assuming a value of $\eta_{L\delta}$ and by computing Ja and Nu_x from Eqs. (46) and (58), respectively.

Following the method of construction described by Churchill and Usag [26], the approximate expression for Nusselt number valid for the whole range of wall subcooling is given by:

$$\frac{Nu_x(2Ja)^{1/2}}{Ra_{x,L}^{1/2}} = \frac{1}{(a)^{1/2}}\left(1 + \frac{2Ja}{\pi}\right)^{1/2} \tag{66}$$

which reduces to the asymptotic expressions given by Eqs. (61) and (64) for small and large wall subcoolings, respectively.

5 Results and discussion

Figure 2a and b show the effects of varying the similarity variable of the dimensionless thickness of the liquid film $\eta_{x,L}$ on the dimensionless velocity profile, for different values of the anisotropic ratio K^* and of the anisotropic orientation φ, respectively. In these figures, it is observed that, when the anisotropic parameters K^* and φ are held constant, each line corresponding to a fixed value of each parameter is a straight line from the origin of the axes, and, as expected, f_L is termed as a linear function of $\eta_{x,L}$. Moreover, it is seen from Fig. 2a that, as K^* is increased from 0.1 to 2.5, for example, when $\varphi = 45°$, the boundary thickness of the liquid film is more and more decreasing. It can be explained from the Eq. (44) that, when the anisotropic parameter $a = \left(cos^2\varphi + K^* sin^2\varphi\right)$ is made more and more higher, the dimensionless velocity profile is decreasing more and more. As a result, the dimensionless thickness of the liquid film is decreasing more and more. This behavior is also observed in Fig. 2b for the varying of φ, when $K^* = 0.1$. It is seen for the same reason that the decreasing in φ corresponds to the decreasing in the dimensionless thickness of the liquid film which becomes more and more weaker.

The dimensionless temperature profile is plotted in Fig. 3a as a function of the similarity variable of the dimensionless thickness of the liquid film $\eta_{x,L}$ to investigate the effects of the anisotropic permeability ratio K^* for two different values of Ja and when the orientation angle of the principal axes of the porous matrix φ is held equal to 45°. As expected, the dimensionless temperature profile decreases first from the unity when $\eta_{x,L} = 0$ about the vertical surface, drops then progressively far away from the surface, become less and less affected by the anisotropic permeability ratio K^* and attains an asymptotic dashed line predicted by Eq. (62). For each value of Ja, it is observed that, the dimensionless temperature profile increases with an increase in the anisotropic permeability ratio K^* for a given value of the dimensionless thickness of the liquid film. So, convection becomes more and more considerable, as K^* is made higher. The same result is obtained in Fig. 3b which illustrates the effect of the orientation anisotropic angle φ and of the Jacob number Ja on the distribution of the temperature θ_L when $K^* = 0.1$. It is seen that, from the reason expressed by the Eq. (45), for a given value of the similarity variable of the dimensionless thickness of the liquid film $\eta_{x,L}$, the temperature in the boundary layer prevailing at the neighborhood of the vertical surface increases with a decrease in the orientation angle of the principal axes of the porous medium.

Figure 4a represents the effects of the anisotropic permeability ratio K^* on the dimensionless film thickness $\eta_{L\delta}$ versus the Jacob number Ja when $\varphi = 45°$. Endeed, Eq. (46) is

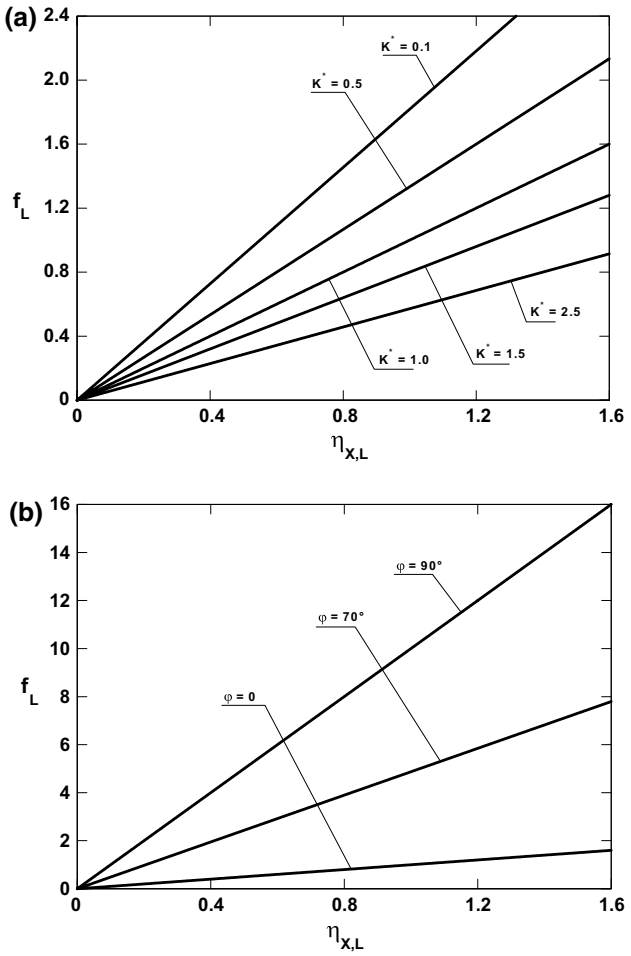

Fig. 2 **a** Effect of varying the similarity variable of the dimensionless thickness of the liquid film $\eta_{x,L}$ on the velocity distribution for various values of the anisotropic ratio K^* when $\varphi = 45°$. **b** Effect of varying the similarity variable of the dimensionless thickness of the liquid film $\eta_{x,L}$ on the velocity distribution for various values of the anisotropic orientation angle φ when $K^* = 0.1$

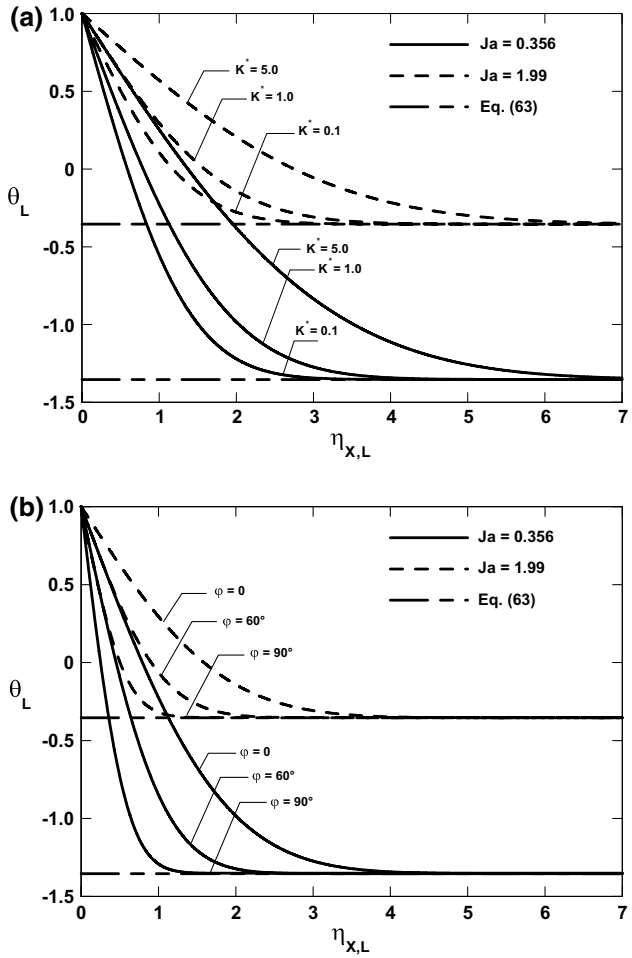

Fig. 3 **a** Effect of varying the similarity variable of the dimensionless thickness of the liquid film $\eta_{x,L}$ on the temperature profile for $Ja = 0.356$ and 1.99 when $\varphi = 45°$ and various values of permeability ratio K^*. **b** Effect of varying the similarity variable of the dimensionless thickness of the liquid film $\eta_{x,L}$ on the temperature profile for $Ja = 0.356$ and 1.99 when $K^* = 0.1$ and various values of the anisotropic orientation angle φ

plotted as solid lines in that figure for various values of K^*. It is noticed that, for a given value of the Jacob number Ja, the dimensionless thickness of the liquid film increases with an increase in K^*. Moreover, for each value of K^*, it is shown that the dimensionless thickness of the liquid film increases as the Jacob number is increased. In the limiting case observed when $\eta_{L\delta} \to 0$, Eq. (59) is plotted as dotted lines in Fig. 4a. Similarly, another view of this trend is to investigate the effects of the orientation anisotropic angle φ and of the Jacob number Ja on the dimensionless film thickness $\eta_{L\delta}$ when K^* is held constant. For example, when $K^* = 0.1$, it is obtained in Fig. 4b that, for a given value of the Jacob number Ja, the dimensionless thickness of the liquid film increases with a decrease in φ from 90° to 0°. Moreover, for each value of φ, it is shown that the dimensionless thickness of the liquid film increases as the Jacob number is increased.

Figure 5a shows the effects of the Jacob number Ja and the anisotropic permeability ratio K^* on the heat transfer rate $Nu_x/Ra_{x,L}^{1/2}$ for $\varphi = 45°$. For a given value of Ja, it is noticed that the heat transfer rate in solid lines increases when K^* is decreasing from 5.0 to 0.1. Also, each curve in solid line drops progressively from a value about $Ja \approx 0$ and goes to a stagnant value which depends on K^*. The asymptotic dotted line to each curve about $Ja \approx 0$ is predicted by Eq. (61) and the asymptotic dashed line to the heat transfer curve far away from the vertical surface is predicted by Eq. (64). The opposite behavior of the heat transfer rate is seen in Fig. 5b where an increase of the latter

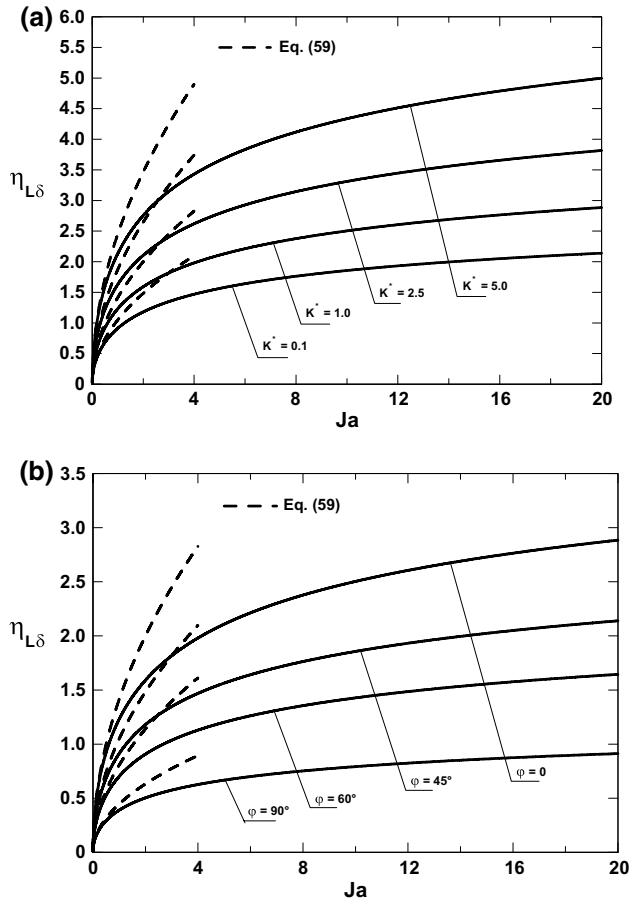

Fig. 4 **a** Effect of varying the Jacob number Ja on the dimensionless film thickness $\eta_{L\delta}$ when $\varphi = 45°$ for various values of the permeability ratio K^*. **b** Effect of varying the Jacob number Ja on the dimensionless film thickness $\eta_{L\delta}$ when $K^* = 0.1$ for various values of the anisotropic orientation angle φ

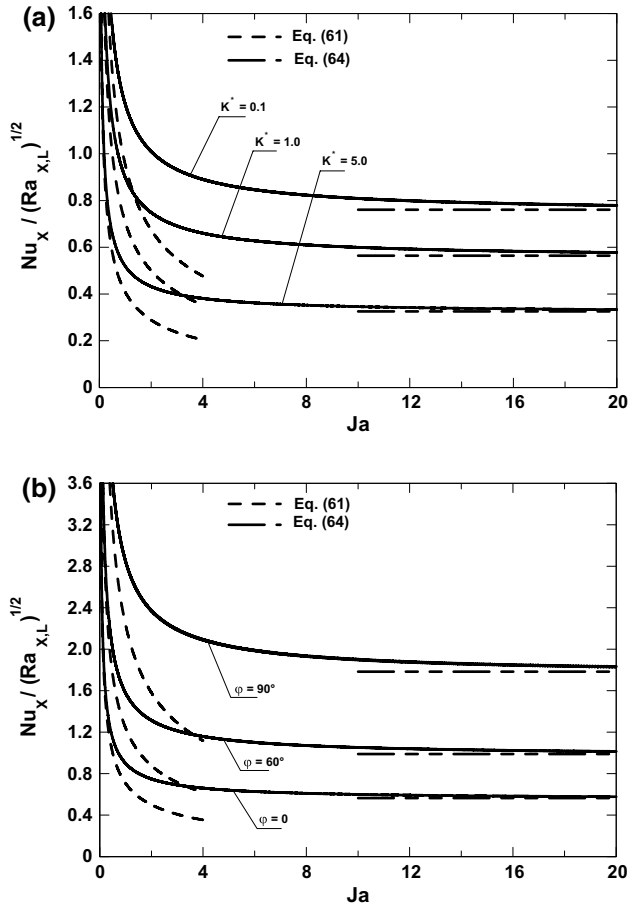

Fig. 5 **a** Effect of the Jacob number Ja on the heat transfer rate $Nu_x/Ra_{x,L}^{1/2}$ when $\varphi = 45°$ for various values of the permeability ratio K^*. **b** Effect of the Jacob number Ja on the heat transfer rate $Nu_x/Ra_{x,L}^{1/2}$ when $K^* = 0.1$ for various values of the anisotropic orientation angle φ

corresponds to an increase of the orientation anisotropic angle φ.

The approximate expression for Nusselt number versus $\left((2Ja)^{1/2}\right)$ given by Eq. (66) which is valid for the whole range of wall subcooling is plotted as solid lines in Fig. 6a to investigate the effects of the anisotropic permeability ratio K^*. The straight (dashed and dotted) lines in Figs. 6a, b are the asymptotic limits of small ($Ja \to 0$) and large ($Ja \to \infty$) wall subcoolings given by Eqs. (61) and (64), respectively. It is seen that, for a given value of $\left((2Ja)^{1/2}\right)$, the heat transfer rate is increased when K^* is decreased from 5.0 to 0.1. Endeed, as expected from Eq. (66), the heat transfer rate is inversely proportional to $\sqrt{a}$, and therefore, inversely proportional to $\sqrt{K^*}$ as $a = cos^2\varphi + K^* sin^2\varphi$ for example, for the particular case when $\varphi = 90°$. It is noticed also that, for the same reason, the heat transfer rate is increased when the orientation of the anisotropic angle is increased from 0° to 90° and when K^* is held equal to 0.1.

6 Conclusions

The problem of film condensation along a vertical surface embedded in a fluid saturated porous medium filled with a dry saturated vapor has been investigated. The porous medium is anisotropic in permeability with its principal axes oriented in a direction that is oblique to the gravity vector. Assuming the usual approximations used in the classical film condensation problems, a similarity solution for the problem is found. Consequently, closed-form expressions of the heat transfer rates and the boundary layer thickness of the condensate are obtained in terms of the Rayleigh number and the anisotropic parameters. The following conclusions are drawn:

1. Both the anisotropic permeability ratio and the anisotropic orientation of the porous matrix have a great influence on the velocity profile, the temperature dis-

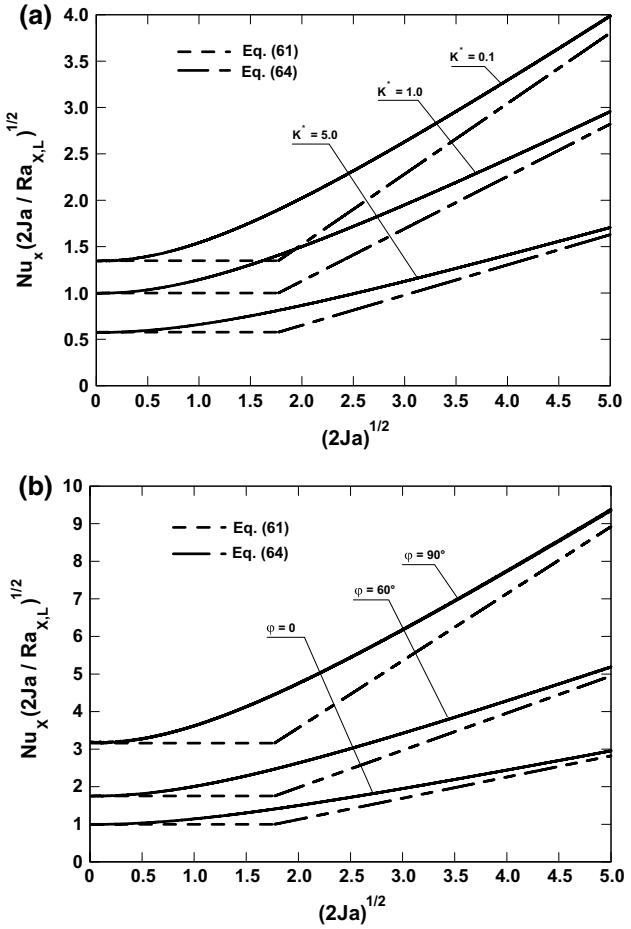

Fig. 6 **a** Effects of the anisotropic permeability ratio K^* on the Nusselt number versus $\left((2Ja)^{1/2}\right)$ when $\varphi = 45°$. **b** Effects of the anisotropic orientation angle φ on the Nusselt number versus $\left((2Ja)^{1/2}\right)$ when $K^* = 0.1$

tribution and the heat transfer in the boundary layer prevailing at the neighborhood of the vertical surface.

2. A decrease in the orientation anisotropic angle corresponds to a decrease in the dimensionless thickness of the liquid film which becomes more and more weaker. Inversely, an increase in the heat transfer rate corresponds to an increase in the orientation anisotropic angle.

References

1. Cheng P (1981) Film condensation along an inclined surface in a porous medium. Int J Heat Mass Transf 14:983–990
2. Liu CY, Ismail KAR, Ebinuma CD (1983) The effect of lateral mass flux on the film condensation in porous medium. Int Commun Heat Mass Transf 10:421–428
3. Kimura S, Bejan A (1984) The boundary-layer natural convection regime in a rectangular cavity with uniform heat flux from the side. J Heat Transf 106:98–103
4. Wang C, Tu C (1989) Boundary-layer flow and heat transfer of non-Newtonian fluids in porous media. Int J Heat Fluid Flow 10:160–165
5. Renken KJ, Aboye M, Carneiro M, Meechan K (1993) Effect of vapor velocity on film condensation along a surface embedded in a porous medium. Int Commun Heat Mass Transf 20:1–13
6. Chiou JS, Chang TB (1994) Laminar film condensation on a horizontal disk with suction at the wall. Comput Math Appl 27(12):61–68
7. Al-Nimr MA, Alkam M (1997) Film condensation on a vertical plate imbedded in a porous. J Appl Energy 56(1):47–57
8. Nield DA, Bejan A (1998) Convection in porous media. Springer, Berlin
9. Kaviany M (1995) Principles of heat transfer in porous media, chapter 12, 2nd edn. Springer, New York, pp 603–675
10. Char MI, Lin JD, Chen HT (2001) Conjugate mixed convection laminar non-Darcy film condensation along a vertical plate in a porous medium. Int J Eng Sci 39:897–912
11. Bautista O, Mendez F, Tamayo P (2006) Conjugate heat transfer analysis of the film condensation on a vertical fin immersed in a porous medium. Mecn Comput XXV:281–296
12. Castinel G, Combarnous M (1974) Critère d'application de la convection naturelle dans une couche poreuse anisotrope. C R Hebd Seanc Acad Sci Paris B B278:701–704
13. Epherre JF (1975) Critère d'application de la convection naturelle dans une couche poreuse anisotrope. Rev Gen Therm 168:949–950
14. Kvernvold O, Tyvand PA (1979) Nonlinear thermal convection in anisotropic porous media. J Fluid Mech 90:609–624
15. Nilsen T, Storesletten L (1990) An analytical study on natural convection in isotropic and anisotropic porous channels. J Heat Transf 112:396–401
16. Kimura S, Masuda Y, Kazuo Hayashi T (1993) Natural convection in an anisotropic porous medium heated from the side (effects of anisotropic properties of porous matrix). Heat Transf Jpn Res 22:139–153
17. Ni J, Beckermann C (1991) Natural convection in a vertical enclosure filled with anisotropic porous media. J Heat Transf 113:1033–1037
18. Zhang X, Nguyen TH, Kahawita R (1993) Convection flow and heat transfer in an anisotropic porous layer with principal axes non-coincident with the gravity vector, vol 264. ASME winter annual meeting, New Orleans, Louisiane, USA. Fundamentals of natural convection-HTD. pp 79–86
19. Degan G, Vasseur P, Bilgen E (1995) Convective heat transfer in a vertical anisotropic porous layer. Int J Heat Mass Transf 38:1975–1987
20. Degan G, Vasseur P (1996) Natural convection in a vertical slot filled an anisotropic porous medium with oblique principal axes. Numer Heat Transf Part A 30:397–412
21. Ene HI (1991) Effects of anisotropy on the free convection from a vertical plate embedded in a porous medium. Transp Porous Media 6:183–194
22. Vasseur P, Degan G (1998) Free convection along a vertical heated plate in a porous medium with anisotropic permeability. Int J Numer Methods Heat Fluid Flow 8:43–63
23. Bear J (1972) Dynamics of fluids in porous media. Dover Publications, New York
24. Bejan A (1984) Convection heat transfer. Wiley, London
25. Ene HI, Polisevsky D (1987) Thermal flow in porous media. D. Reidel, Dordrecht
26. Churchill SW, Usag R (1972) A general expression for the correlation of rates of transfer and other phenomena. AIChE J 18:1121–1128